Surface response in the Fermi-liquid drop and nuclear transport properties

A. G. Magner,[1,2] V. M. Kolomietz,[1-3] H. Hofmann,[2] and S. Shlomo[3]

[1] *Institute for Nuclear Research, 252022 Kiev, Ukraine*
[2] *Physik-Department TU München, 85747 Garching, Germany*
[3] *Cyclotron Institute, Texas A&M University, College Station, Texas 77843*

Response functions for isoscalar multipole excitations are calculated for a large range of temperatures and analyzed in terms of transport coefficients. The dynamics of the nucleons is treated semiclassically by applying the collisional Landau-Vlasov equation for the interior region, supplemented by the "effective nuclear surface approximation" introduced previously to describe the dynamics of the surface. Collisions are considered in modified relaxation time approximation with a temperature- and frequency-dependent relaxation time. The strength distribution shows a marked transition from the zero sound like behavior at small temperatures to the one corresponding to collision dominated modes. The latter appear at small frequencies and are underdamped. Within our present model the transition occurs at large temperatures of about $T \geq 4$ MeV. For the intermediate temperatures the overdamped modes are found as related to the low-lying peaks in the strength function. The results are illustrated by the calculations of the strength function for the quadrupole excitations in the nucleus ^{208}Pb.

I. INTRODUCTION

Collective motion at finite excitations still is not completely understood. One would commonly expect it to be governed by "macroscopic" features, the more so the larger the excitation is. Traditionally the macroscopic description of average static and dynamic characteristics of nuclei has been based on the classical liquid drop model (LDM) [1,2]. On the other hand it should be apparent that the specific properties characteristic of Fermi liquids cannot be discarded [3,4] when we want to describe a nucleus as a finite drop. One property of this type, for instance, is the dynamical distortion of the Fermi surface [5–7] accompanying collective motion.

Collective dynamics of a Fermi liquid can be described within the phase-space approach which is based on the semiclassical collisional Landau-Vlasov equation; see Refs. [5,8]. Specific problems appear for small finite systems like a nucleus where in the surface region a semiclassical description becomes doubtful. However, as shown in Ref. [9], this difficulty may eventually be circumvented by making use of the "effective nuclear surface approximation." The latter uses a special leptodermous expansion in the smallness parameter $a/R \approx A^{-1/3}$, where a stands for the thickness of the diffuse edge and R is the nuclear radius. One may then define the effective nuclear surface as the position of the maxima of the time-dependent spatial gradient of the particle density. In this way one can split the dynamic problem into two parts: (i) For the interior region, where relatively small dynamic oscillations of the particle density take place, one may apply the semiclassical Landau-Vlasov equation. One may even go one step further and translate this equation for the distribution function into a set of equations for the physically observed quantities such as

the particle density, current, and pressure tensor. This has been demonstrated in Ref. [10] for the case of small amplitude vibrations. (ii) In the nuclear edge, instead of solving a very complicated dynamical problem, one may use simple macroscopic boundary conditions for the previously mentioned observed quantities. These boundary conditions, together with the continuity equations for particle number and momentum, reflect similarities to the standard dynamic problem of the classical hydrodynamics [11]. We will consider the properties of the nuclear resonances as functions of temperature. These properties were studied earlier in Refs. [12,13] within the framework of the quantum response theory. Such kinds of investigations are interesting also in connection with averaging procedures of the nuclear responses considered in Refs. [14,15].

In Sec. II we shall exhibit some of the basic properties of the Landau Fermi-liquid theory as applied to a finite drop. We then continue to derive in Sec. III response functions for collective vibrations. Their interpretation in terms of transport theory is given in Sec. IV. The discussion of numerical results will be presented in Sec. V.

II. FERMI-LIQUID DROP MODEL (FLDM)

We shall consider below small vibrations of the nuclear surface near a spherical shape, which are induced by an external field $V_{\rm ext}(t)$. To this end we introduce a collective variable $Q(t)$ in the usual way,

$$R = R_0[1 + Q(t)Y_{l0}(\hat{r})], \qquad (2.1)$$

where R_0 is the equilibrium radius of the nucleus and

$Y_{l0}(\hat{r})$ are the spherical harmonics representing axially symmetric shapes. For $Q(t)$ we will assume the form

$$Q(t) = Q_\omega e^{-i\omega t}. \tag{2.2}$$

A. Equations of motion inside the nucleus

In the nuclear volume, where variations of the density $\varrho(\vec{r}, t)$ are small, the quasiparticle concept of the Landau-Fermi-liquid theory [5] can be justified. Therefore in the interior of sufficiently heavy nuclei one may describe the particle phase-space dynamics in a semiclassical approximation in terms of the distribution function $f(\vec{r}, \vec{p}, t)$ which is obtained as a solution to the collisional Landau-Vlasov equation

$$\frac{\partial}{\partial t}\delta f + \frac{\vec{p}}{m^*}\vec{\nabla}_r\delta f - \vec{\nabla}_r\delta V^W \cdot \vec{\nabla}_p f_{\rm eq} - \delta St(f) = 0. \tag{2.3}$$

Here $V^W \equiv V^W(\vec{r}, \vec{p}, t)$ stands for the Wigner transform of the mean field V, which in principle should include $V_{\rm ext}(t)$. However, we will assume that the external field is concentrated in the nuclear surface and will thus include $V_{\rm ext}(t)$ in the boundary conditions. The variation $\delta f(\vec{r}, \vec{p}, t)$ in Eq. (2.3) is the dynamic component of the distribution function

$$f = f_{\rm eq} + \delta f, \tag{2.4}$$

where $f_{\rm eq}$ is the Fermi distribution function,

$$f_{\rm eq} = \left[1 + \exp\frac{\epsilon_{\rm eq} - \lambda}{T}\right]^{-1}, \tag{2.5}$$

for the equilibrium inside the nucleus. Here, $\epsilon_{\rm eq} = p^2/2m^*$, m^* is the effective nucleon mass, λ is the chemical potential, and T is the nuclear temperature; $\lambda \approx \epsilon_F =$

$p_F^2/2m^*$ for $T \ll \epsilon_F$, where ϵ_F is the Fermi energy and p_F is the Fermi momentum. The quantity $\delta V^W(\vec{r}, \vec{p}, t)$ in Eq. (2.3) is the Wigner transform of the variation of the self-consistent potential

$$V^W = V_{\rm eq} + \delta V^W, \tag{2.6}$$

where $V_{\rm eq}$ is the equilibrium mean field which is approximately constant for the nuclear interior. The dynamic component δV^W is expressed in terms of the interaction amplitude $\mathcal{F}(\vec{p}, \vec{p}')$ as

$$\delta V^W = \frac{2}{N_F}\int\frac{d\vec{p}'}{(2\pi\hbar)^3}\mathcal{F}(\vec{p}, \vec{p}')\delta f(\vec{r}, \vec{p}'; t), \tag{2.7}$$

where $N_F = p_F m^*/(\pi^2\hbar^3)$. The quantity $\mathcal{F}(\vec{p}, \vec{p}')$ is usually parametrized in terms of the Landau constants $\mathcal{F}_0$ and $\mathcal{F}_1$ as

$$\mathcal{F}(\vec{p}, \vec{p}') = \mathcal{F}_0 + \mathcal{F}_1\hat{p}\cdot\hat{p}', \quad \hat{p} = \vec{p}/p. \tag{2.8}$$

These constants are related to the incompressibility modulus K of nuclear matter and effective nucleon mass m^* by

$$K = 6\epsilon_F(1 + \mathcal{F}_0), \tag{2.9}$$

$$m^* = m\left(1 + \frac{1}{3}\mathcal{F}_1\right), \tag{2.10}$$

where m is the nucleon mass.

In Eq. (2.3), $\delta St(f)$ denotes the collision term which we shall consider in the τ approximation [5], modified, however, by the frequency and the temperature dependence of the "collision time" τ. This dependence follows from the generalized τ approximation considered in Refs. [6,7,10,16],

$$\delta St(f) = \frac{1}{\tau}\left\{\delta f(\vec{r}, \vec{p}, t) - \int d\Omega_k A(\hat{k})[\alpha_0 Y_{00} + \alpha_1 Y_{10}(\hat{p}\cdot\hat{k})]\frac{\partial f_{\rm eq}(\epsilon)}{\partial\epsilon}\bigg|_{\epsilon=\epsilon_{\rm eq}}\exp[i(\vec{k}\cdot\vec{r} - \omega t)]\right\}, \tag{2.11}$$

where $\delta f(\vec{r}, \vec{p}, t)$ is considered as a superposition of plane sound waves of amplitude $A(\hat{k})$,

$$\delta f(\vec{r}, \vec{p}, t) = \int d\Omega_k A(\hat{k})\tilde{f}(\hat{p}\cdot\hat{k})\frac{\partial f_{\rm eq}(\epsilon)}{\partial\epsilon}\bigg|_{\epsilon=\epsilon_{\rm eq}}\exp[i(\vec{k}\cdot\vec{r} - \omega t)], \tag{2.12}$$

$$\tilde{f}(\hat{p}\cdot\hat{k}) = \sum_L \alpha_L(\omega, k)Y_{L0}(\hat{p}\cdot\hat{k}), \quad \hat{k} = \vec{k}/k. \tag{2.13}$$

The relaxation time τ in Eq. (2.11) is assumed to be frequency dependent. Following Ref. [10] we take the form

$$\tau = \frac{\tau_0}{T^2 + \zeta(\hbar\omega)^2}. \tag{2.14}$$

Formula (2.14) has been derived in Ref. [10] by inte-

grating Eq. (2.3) over $\epsilon_{\rm eq}$, assuming that for $\hbar\omega \ll \lambda$ and $T \ll \lambda$ the derivative of the equilibrium distribution function $f_{\rm eq}(\epsilon_{\rm eq})$ over its argument is sharply peaked at λ and that the interaction amplitude $\mathcal{F}(\vec{p}, \vec{p}')$ of Eq. (2.8) can be parametrized only by two constants $\mathcal{F}_0$ and $\mathcal{F}_1$. In this case $\zeta = 3/4\pi^2$. We point out that the inclusion of memory effects in the relaxation time was also considered in Refs. [17–19]. Using the attenuation coefficient approach of Landau [5,20], a value of $\zeta = 1/4\pi^2$ was obtained in Ref. [19]. Formula (2.14) may in some sense

be compared with expressions suggested in Ref. [21] for the imaginary part of the self-energy to be used in microscopic computations like those of Refs. [13,12,21]. This form, however, differs in a twofold sense: Besides the $3/4\pi^2$ another parameter was considered which weakens the dependence on both ω and temperature T at large values of these quantities.

Let us transform the Landau-Vlasov equation (2.3) to equations for the $\vec{p}$ moments of the distribution function $f(\vec{r}, \vec{p}; t)$, like the continuity equation

$$\frac{\partial}{\partial t}\delta\rho + \rho_{\rm eq}\vec{\nabla}\cdot\vec{U} = 0, \qquad (2.15)$$

the equation for momentum conservation

$$m\rho_{\rm eq}\frac{\partial U_\alpha}{\partial t} + \sum_\beta \frac{\partial}{\partial r_\beta}\delta\Pi_{\alpha\beta} = 0, \qquad (2.16)$$

etc.; see Ref. [8]. In Eqs. (2.15) and (2.16), U_α are the Cartesian components of the mean velocity field,

$$U_\alpha(\vec{r},t) = \frac{2}{(2\pi\hbar)^3\rho_{\rm eq}}\int d\vec{p}\,\frac{p_\alpha}{m}\delta f(\vec{r},\vec{p};t), \qquad (2.17)$$

and $\delta\rho$ is given by

$$\delta\rho(\vec{r},t) = \frac{2}{(2\pi\hbar)^3}\int d\vec{p}\,\delta f(\vec{r},\vec{p};t) \propto Y_{l0}(\hat{r}), \qquad (2.18)$$

where the proportionality to the spherical harmonics is

due to the following choice of the amplitude:

$$A(\hat{k}) = Y_{l0}(\hat{k}), \qquad (2.19)$$

which we are going to apply to describe vibrations of multipolarity l. Following Ref. [10], we can represent the dynamic part of the momentum flux tensor $\delta\Pi_{\alpha\beta}$ in Eq. (2.16) as

$$\delta\Pi_{\alpha\beta} = \frac{K}{9}\delta\rho\delta_{\alpha\beta} - \mu\left[\frac{\partial W_\alpha}{\partial r_\beta} + \frac{\partial W_\beta}{\partial r_\alpha} - \frac{2}{3}\vec{\nabla}\cdot\vec{W}\delta_{\alpha\beta}\right]$$
$$-\nu\left[\frac{\partial U_\alpha}{\partial r_\beta} + \frac{\partial U_\beta}{\partial r_\alpha} - \frac{2}{3}\vec{\nabla}\cdot\vec{U}\delta_{\alpha\beta}\right], \qquad (2.20)$$

where $\vec{W}$ is the displacement field,

$$\vec{U} = \frac{\partial}{\partial t}\vec{W}, \qquad (2.21)$$

μ is the Fermi surface distortion parameter,

$$\mu = \frac{3}{2}\frac{\rho_{\rm eq}\lambda}{G_1}\left[\mathrm{Re}(S^2) - \frac{G_0 G_1}{3}\right], \qquad (2.22)$$

and ν is the viscosity coefficient,

$$\nu = -\frac{3}{2}\frac{\rho_{\rm eq}\lambda}{\omega G_1}\mathrm{Im}\,(S^2), \qquad (2.23)$$

with $G_0 = 1 + \mathcal{F}_0$ and $G_1 = 1 + \mathcal{F}_1/3$. The quantities $\omega\tau$ and S are connected to each other by the dispersion relation (see Ref. [5])

$$\frac{i\omega\tau}{i\omega\tau - 1}G_1 - Q_1(\xi)\left\{G_1\left(\mathcal{F}_0 - \frac{1}{i\omega\tau - 1}\right) + \xi^2\left(\mathcal{F}_1 - \frac{3}{i\omega\tau - 1}\right)\frac{i\omega\tau}{i\omega\tau - 1}\right\} = 0. \qquad (2.24)$$

Here, k is the wave number,

$$\xi = S\left(1 + \frac{i}{\omega\tau}\right), \quad S = \frac{\omega}{v_F k}, \quad v_F = \frac{p_F}{m^*}, \qquad (2.25)$$

and

$$Q_1(\xi) = \frac{1}{2}\int_{-1}^{1}\frac{dx\,x}{\xi - x} \qquad (2.26)$$

is the Legendre function of the second kind. Substituting the relation

$$\lim_{\xi_I\to+0}\frac{1}{x - \xi_R - i\xi_I} = \mathcal{P}\left(\frac{1}{x - \xi_R}\right) + i\pi\delta(x - \xi_R) \qquad (2.27)$$

into the integral (2.26) and comparing with the explicit expression for this integral for $\xi_I \to +0$ gives the definition of the physical sheet of the many-valued logarithmic function, which appears in Eq. (2.26) in the complex

plane of the variable ξ. This definition corresponds to the well-known Landau rule to avoid the pole singularity [20].

We emphasize that we have not employed any truncation scheme for the moments of Eq. (2.3) in deriving the equations of motion (2.15), (2.16), and (2.20). However, our approach involved the somewhat complicated dispersion relation (2.24), which was derived directly from Eq. (2.3). This is to be contrasted with the common fluid dynamic approach (see Refs. [3,22–32]), in which a truncation of the equations of moments of (2.3) is achieved by restricting the value of the multipolarity of the dynamical Fermi-surface distortion. We also add that our approach is more adequate for the description of the zero-sound regime and for the transition to the hydrodynamical regime in the case of small values for the Landau interaction parameter F_0 which is usually used in nuclear Fermi liquid.

From Eqs. (2.12)–(2.14), (2.17), and (2.19) one gets

$$\vec{U} = \vec{\nabla}\varphi, \qquad (2.28)$$

where

$$\varphi = \frac{1 + \mathcal{F}_1/3}{p_F} \frac{\alpha_1}{ik} \sqrt{\frac{3}{4\pi}} \int d\Omega_k Y_{l0}(\hat{p} \cdot \hat{k}) \exp[i(\vec{k} \cdot \vec{r} - \omega t)].$$

(2.29)

With Eq. (2.28), Eqs. (2.15) and (2.16) are reduced to one equation for the potential φ,

$$m\varrho_{\text{eq}} \frac{\partial^2 \varphi}{\partial t^2} - \frac{1}{9}\left(K + \frac{12\mu}{\varrho_{\text{eq}}}\right)\varrho_{\text{eq}}\Delta\varphi - \frac{4}{3}\nu\Delta\frac{\partial\varphi}{\partial t} = 0.$$

(2.30)

B. Boundary conditions and external field

The dynamics in the surface layer of the nucleus can be described by means of the macroscopic boundary conditions derived in Ref. [33], using the effective surface approximation [9]. For small vibration amplitudes they read

$$U_r\big|_{r=R_0} = \dot{R}(t) = R_0\dot{Q}(t)Y_{l0}(\hat{r}),$$

(2.31)

$$\delta\Pi_{rr}\big|_{r=R_0} = \delta P_S + P_{\text{ext}},$$

(2.32)

where U_r and $\delta\Pi_{rr}$ are the radial components of the velocity field $\vec{U}$, Eq. (2.17), and momentum flux tensor $\delta\Pi_{\alpha\beta}$, Eq. (2.20), respectively, which are determined in the nuclear volume. The boundary conditions (2.31) and (2.32) adopted here are the common ones which are used for small vibrations in a finite liquid; see Ref. [11]. These conditions are similar to those used in Refs. [27–29] for nuclear fluid dynamics. We note that the effects of the surface tension were ignored in Refs. [27–29]. The surface pressure δP_S which is due to the tension forces [1] is given by

$$\delta P_S = \frac{\sigma}{R_0}(l-1)(l+2)Q(t)Y_{l0}(\hat{r}),$$

(2.33)

where σ is the tension coefficient. Here and below we neglect the relatively small corrections of the order of $A^{-1/3}$, which are related to the external field.

In Eq. (2.32) there appears an external pressure P_{ext}. It is here where we make connection to the external potential V_{ext} we spoke of before by writing

$$P_{\text{ext}} = \int_0^\infty dr\ \rho_{\text{eq}}(r)\frac{\partial V_{\text{ext}}}{\partial r}.$$

(2.34)

For the density in equilibrium which appears in Eq. (2.34) we take the form

$$\rho_{\text{eq}}(r) = \rho_0 y(R - r),$$

(2.35)

expressed in terms of the profile function $y(x)$ which we are going to approximate by a step function. The ρ_0 is the value of equilibrium density inside the nucleus, i.e.,

$\rho_0^{-1} = (4\pi/3)r_0^3$, and $R_0 = r_0 A^{1/3}$ is the nuclear radius. We will assume that the external field

$$V_{\text{ext}}(\vec{r}, t) = q_{\text{ext}}(t)\hat{F}(\vec{r})$$

(2.36)

is concentrated in the surface region of the nucleus. For $\hat{F}(\vec{r})$ we take the form

$$\hat{F}(\vec{r}) = -\left(\frac{\delta V}{\delta\rho}\right)_{\text{eq}} R_0\left(\frac{\partial\rho_{\text{eq}}}{\partial r}\right)_{R=R_0} Y_{l0}(\hat{r}).$$

(2.37)

After substitution of Eqs. (2.35) and (2.37) into Eq. (2.34) we have

$$P_{\text{ext}} = -\frac{\kappa}{R_0^3}q_{\text{ext}}(t)Y_{l0}(\hat{r}),$$

(2.38)

where

$$\kappa = -\left(\frac{\delta V}{\delta\rho}\right)_{\text{eq}}\frac{\sigma R_0^4}{2\beta}.$$

(2.39)

Here β is the coefficient which in the nuclear energy density formula appears in front of the term which is proportional to $[\vec{\nabla}\rho_{\text{eq}}(r)]^2$. From Refs. [4,34], we have $\beta=70$–90 MeV fm^5. Both in the definition (2.37) of $\hat{F}$ as well as in the constant κ the functional derivative of the mean field with respect to the density appears. Within our linearized approach this derivative has to be evaluated at the equilibrium density. It may be noted that these features are similar to the ones discussed in Ref. [1] for finite nuclei. In a future paper, which is to be published elsewhere, this similarity will be worked out in more detail. Here we may just note that the factor $(\delta V/\delta\rho)_{\text{eq}}$ finally drops out of all physical quantities we are going to discuss below. For the tension coefficient we have used an expression found in Ref. [34] within the "sharp surface approximation" [9]

$$\sigma \approx 2\beta \int_0^\infty dr\left(\frac{\partial\rho_{\text{eq}}}{\partial r}\right)^2.$$

(2.40)

III. RESPONSE FUNCTION

Let us write the linearized dynamic part of the nucleonic density $\delta\rho(\vec{r}, t)$ as a sum of a "volume" and a "surface" term,

$$\delta\rho(\vec{r}, t) = \delta\rho^{\text{vol}}(\vec{r}, t)y(R_0 - r) - \frac{\partial y(R_0 - r)}{\partial r}\rho_0\delta R,$$

(3.1)

where δR is the variation of the nuclear radius,

$$\delta R = R_0 Q(t)Y_{l0}(\hat{r}).$$

(3.2)

The upper index "vol" in $\delta\rho^{\text{vol}}(\vec{r}, t)$ of Eq. (3.1) indicates that this quantity is determined by the equation of motion in the nuclear volume and is given in terms of the distribution function $\delta f(\vec{r}, \vec{p}; t)$ through Eq. (2.18). Solving Eq. (2.30) with the first boundary condition (2.31),

one gets the potential φ of Eq. (2.28) in the form

$$\varphi(\vec{r}, t) = \frac{1}{k^2} \frac{kR_0}{j_l'(kR_0)} \dot{Q}(t) j_l(kr) Y_{l0}(\hat{r}), \qquad (3.3)$$

where $j_l(x)$ is the spherical Bessel function and $j_l'(x) = dj_l(x)/dx$. From the continuity equation (2.15) with Eqs. (2.28) and (3.3) one has

$$\delta\rho^{\text{vol}}(\vec{r}, t) = \rho_0 \frac{kR_0}{j_l'(kR_0)} Q(t) j_l(kr) Y_{l0}(\hat{r}). \qquad (3.4)$$

Therefore according to Eqs. (3.1), (3.2), and (3.4) one finds that

$$\delta\rho(\vec{r}, t) = \rho_0 Q(t) Y_{l0}(\hat{r}) \left[\frac{kR_0}{j_l'(kR_0)} j_l(kr) y(R_0 - r) \right.$$
$$\left. - \frac{\partial y(R_0 - r)}{\partial r} R_0 \right]. \qquad (3.5)$$

For the monopole case the conservation law for particle number, $\int d\vec{r}\delta\rho = 0$, is fulfilled identically in k because Eq. (2.31) leads to a cancellation between the contribution of the "volume" part and the contribution of the "surface" part of $\delta\rho(\vec{r}, t)$ in Eq. (3.5).

With this solution we may now proceed to calculate the response function $\chi(\omega)$ which measures how the average of $\hat{F}$ changes with the external field of Eqs. (2.36) and (2.37). Expressed in terms of the Fourier transform $\delta\rho_\omega(\vec{r})$ of the transition density $\delta\rho(\vec{r}, t)$ it can be defined [2,4,13,35] as

$$\chi(\omega) = -\frac{1}{q_{\text{ext}}^\omega} \int d\vec{r}\hat{F}(\vec{r})\delta\rho_\omega(\vec{r}), \qquad (3.6)$$

where q_{ext}^ω is the Fourier component of the external field [see Eq. (2.36)],

$$q_{\text{ext}}(t) = q_{\text{ext}}^\omega e^{-i(\omega + i\epsilon)t}, \quad \epsilon = +0. \qquad (3.7)$$

We may express the response function in terms of our collective variable Q. Indeed, substituting the Fourier transform of Eq. (3.5) together with $\hat{F}$ from Eq. (2.37)

into Eq. (3.6) we obtain

$$\chi(\omega) = \kappa Q_\omega / q_{\text{ext}}^\omega, \qquad (3.8)$$

with the Q_ω given by Eq. (2.2).

Using Eqs. (2.20), (2.21), (2.28), (2.33), and (3.3) one may write the equation of motion (2.32) in terms of the collective variable $Q(t)$ and periodic time dependence of the external field V_{ext} in the form

$$\mathcal{B}_l(x)\ddot{Q} + \mathcal{C}_l(x)Q + \mathcal{Z}_l(x)\dot{Q} = -\kappa q_{\text{ext}}. \qquad (3.9)$$

We have introduced in this equation various new quantities, such as

$$x = \frac{\omega R_0}{v_F S}, \qquad (3.10)$$

which by means of Eqs. (2.24) and (2.25) is a complex function of ω, as well as the quantities

$$\mathcal{B}_l(x) = m\rho_0 R_0^5 \frac{j_l(x)}{x j_l'(x)}, \qquad (3.11)$$

$$\mathcal{C}_l(x) = C_l^{(S)} + \mathcal{C}_l^{(\mu)}(x), \qquad (3.12)$$

$$C_l^{(S)} = \sigma R_0^2 (l - 1)(l + 2), \qquad (3.13)$$

$$\mathcal{C}_l^{(\mu)} = 2\mu R_0^3 \frac{x}{j_l'(x)} [j_l''(x) + j_l(x)], \qquad (3.14)$$

and

$$\mathcal{Z}_l(x) = 2\nu R_0^3 \frac{x}{j_l'(x)} [j_l''(x) + j_l(x)]. \qquad (3.15)$$

From Eq. (3.9) one has

$$\frac{Q_\omega}{q_{\text{ext}}^\omega} = \frac{\kappa}{g_l(x)} \qquad (3.16)$$

with

$$g_l(x) = -\left[\mathcal{B}_l(x)\omega^2 - \mathcal{C}_l(x) + i\omega\mathcal{Z}_l(x)\right]$$
$$= \frac{C_l^{(S)}}{j_l'(x)} \left\{ j_l'(x) - \frac{6A^{1/3}\lambda x}{b_S(l-1)(l+2)} \left[\left(-\frac{\mu}{\rho_0\lambda} + i\frac{\nu v_F}{\rho_0\lambda R_0}xS\right) j_l''(x) + \left(\frac{S^2}{G_1} - \frac{\mu}{\rho_0\lambda} + i\frac{\nu v_F}{\rho_0\lambda R_0}xS\right) j_l(x)\right] \right\}, \qquad (3.17)$$

where $b_S = 4\pi r_0^2\sigma \approx 17$ MeV and $r_0 = 1.2$ fm. In a realistic situation the value of r_0 is a little smaller, when related to the correct particle density ρ_0, but the results of the calculations in FLDM are not sensitive to small changes in r_0. So the response function $\chi(\omega)$ defined in

Eq. (3.8) is written with the help of Eq. (3.16) as

$$\chi(\omega) = \frac{\kappa^2}{g_l(x(\omega))}. \qquad (3.18)$$

The poles of the collective response function (3.18) are determined by the following equation:

$$g_l(x) = -\mathcal{B}_l(x)\omega^2 + \mathcal{C}_l(x) - i\omega\mathcal{Z}_l(x) = 0. \quad (3.19)$$

This is the secular equation to the dispersion relation (2.24). Using Eqs. (2.25) and (3.10) we find a discrete sequence of roots of Eq. (3.19) which we denote by

$$\omega = \pm\omega_n - i\Gamma_n, \quad n = 0, 1, ..., \quad (3.20)$$

with $\Gamma_n > 0$. Note that we want to concentrate on stable modes. The enumeration of the modes will be done such that the magnitude of ω_n increases with n. We will consider roots with ω_n being in the frequency region of about $\hbar\omega \le 2\hbar\Omega$, which overlaps with the energy of the giant quadrupole resonance discussed below. The characteristic frequency Ω represents the gross shell spacing. It can be estimated by

$$\Omega = \frac{v_F}{R_0} \sim \frac{\lambda}{A^{1/3}\hbar}, \quad (3.21)$$

the characteristic frequency in which a particle with energy near λ traverses a mean potential well of radius R_0. For such a frequency regime the quasiparticle concept of Landau's Fermi-liquid theory can be applied. Since only the lowest two solutions associated with $n = 0$ and 1 of the infinite sequence (3.20) lie in this frequency region of $\hbar\omega \le 2\hbar\Omega$, we will henceforth concentrate on them.

Let us first look at the root denoted by $n = 1$ with the real part being larger than the imaginary part; see the lower part of Fig. 1. At zero temperature this pole lies near the real axis. It can be interpreted as a zero-sound mode with $\omega\tau \gg 1$ and corresponds to the giant multipole resonance. The characteristic equation (3.19) coincides with the one obtained in Ref. [10]. The quantities ω_n and Γ_n are functions of the temperature T through the solution $S = S(\omega\tau)$ of the dispersion equation (2.24); see also the relation (2.14). With increasing temperature T the pole associated with $n = 1$ is shifted to the low-frequency region where $\omega\tau$ becomes small, $\omega\tau \ll 1$, such that we have a transition from the zero-sound regime to the hydrodynamic one dominated by collisions; see Figs. 1 and 2. In this limit of $\omega\tau \to 0$, Eq. (3.19) reduces to the characteristic equation of classical hydrodynamics similar to the case discussed in Ref. [1] for undamped motion. For all temperatures the pole associated with $n = 1$ is related to the excitations of the underdamped mode with Γ_1 being smaller than or of the order of ω_1.

The other pole associated with $n = 0$ is purely imaginary and represents overdamped motion. In principle, also for overdamped motion the solutions of Eq. (3.19) can be grouped in pairs (see Appendix B). However, in the sequel we want to concentrate on situations of large damping. In this case one of the two poles falls out of the regime $\hbar\omega \le 2\hbar\Omega$ so that it can safely be neglected. The other pole, which will be taken into account, lies at $\omega = -i\Gamma_0$ [with $\omega_0 = 0$ following the notation of Eq. (3.20)]. The value of Γ_0 can be found analytically, at least if we concentrate on the most important frequency region of about $|\omega| \le S_{\mathrm{LD}}\Omega \approx \Omega$. This condition implies

that we have $|x| < 1$ because $|S| \ge S_{\mathrm{LD}} = \sqrt{G_0 G_1/3}$, where S_{LD} is the first sound velocity; see Refs. [6,7,16]. By taking into account the rapid convergence of the expansion of the Bessel functions $j_l(x)$ in powers of x for $|x| < 1$ and Eqs. (2.22) and (2.23), we note that the solution of Eq. (3.19) with $n = 0$ corresponds to the hydrodynamic regime with small $|\omega\tau|$. The quantity S can be approximated by the following expression found in Refs. [6,7] by looking for a perturbation expansion in the parameter $\omega\tau$:

$$S = S_{\mathrm{LD}} - \frac{2G_1}{15S_{\mathrm{LD}}} i\omega\tau. \quad (3.22)$$

The quantity S is real due to the pure imaginary value of ω in the overdamped pole, contrary to the $n = 1$ mode for which S is a complex number [36]. By making use of the perturbation expansion (3.22) in $\omega\tau$ and Eq. (3.19) we obtain, for the Γ_0 of the overdamped pole,

$$\omega = -i\Gamma_0, \quad (3.23)$$

the expression

$$\Gamma_0 = \frac{5b_S(l-1)(l+2)}{12A^{1/3}\lambda\tau} \approx \frac{5b_S(l-1)(l+2)}{12A^{1/3}\lambda\tau_0}T^2. \quad (3.24)$$
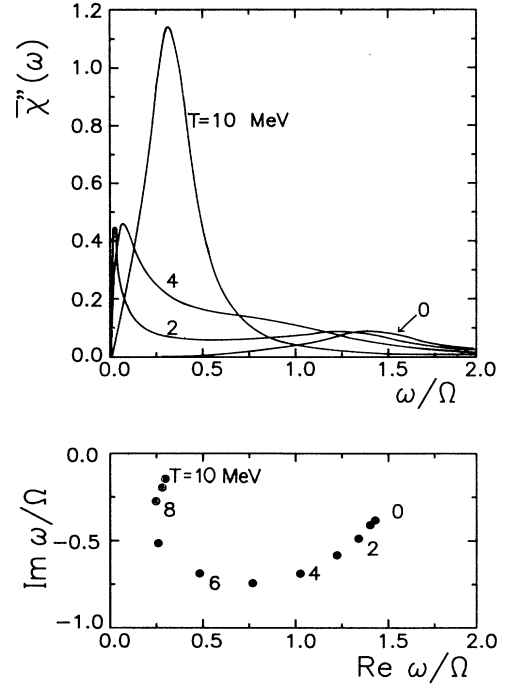
FIG. 1. The response function $\bar{\chi}''(\omega)$ from Eq. (5.1) versus the frequency ω/Ω in units of Ω, Eq. (3.21), for the quadrupole vibrations. The different curves correspond to the temperatures $T = 0$, 2, 4, and 10 MeV. We have used the values of $\epsilon_F = 40$ MeV, $b_S = 17$ MeV, $A = 208$, $r_0 = 1.2$ fm, $\mathcal{F}_0 = -0.2$, $\mathcal{F}_1 = 0.6$, and $\tau_0 = (30/\Omega)$ MeV². The underdamped ($n = 1$) poles are shown by solid dots for different temperatures in the bottom of the figure.
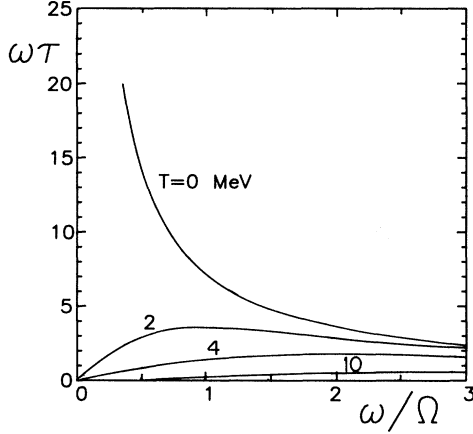
FIG. 2. The function $\omega\tau(\omega)$ plotted versus ω/Ω with $\tau_0 = (30/\Omega)$ MeV^2.

In the second equation we assumed that the temperature T is sufficiently large so that we can neglect the ω dependence of the relaxation time τ in Eq. (2.14). The approximate solution (3.24) was found for heavy nuclei with a particle number of about $A \geq 100$. The A dependence $\Gamma_0 \propto A^{-1/3}$ in Eq. (3.24) is in contrast to the typical two-body collision behavior of $A^{-2/3}$. This is a peculiarity of the overdamped mode. The damping of this mode is directly related to the boundary conditions (2.31) and (2.32) through $\Gamma_0 \propto b_S \propto \sigma$ and in this respect it is similar to the one-body dissipation where $\Gamma_{\text{one body}} \propto A^{-1/3}$; see Ref. [3]. This overdamped mode is specifically related to the finite size of the system and in principle has no analogous mode in infinite nuclear matter. This is in contrast with the underdamped volume mode where $\Gamma \propto \omega^2$ and the $A^{-2/3}$ dependence is due to the $A^{-1/3}$ dependence of ω. The τ dependence $\Gamma_0 \propto \tau^{-1}$ is similar to the one for the collisional width of a giant resonance in the zero-sound regime; see Ref. [10]. In a general case, the width Γ_n of the giant resonance may be due to both sources: two-body collisions and Landau damping (the escape width, which is relatively small for heavy nuclei, is not taken into account in our approach). Landau damping is included in our approach through the dispersion relation (2.24) derived in the Landau theory of the Fermi liquid; see Ref. [5]. However, it contributes to Γ_n only when the complex roots of Eq. (2.24) are on the physical sheet. A detail analysis of the Landau damping contribution to Γ_n and its relation to one-body dissipation phenomena will be given in a separate publication. Here, we have concentrated on the temperature behavior of the Fermi-liquid response function and on the low-lying overdamped mode.

IV. TRANSPORT PROPERTIES

The macroscopic response of a system to an external field allows us to introduce the transport coefficients. We

follow Ref. [37] and first rewrite the equation of motion (3.9) for the collective variable $Q(t)$ in the form of an energy conservation law as

$$\frac{d}{dt}\left[\frac{1}{2}M_l\dot{Q}_R^2 + \frac{1}{2}C_lQ_R^2\right] + \gamma_l\dot{Q}_R^2 = -\kappa q_{\text{ext}}^{(R)}(t)\dot{Q}_R. \quad (4.1)$$

Here we have taken the real part of Eq. (3.9) and specified to the physical velocity of the surface as a real quantity: $\dot{Q}_R(t) = \text{Re } \dot{Q}(t)$ and $q_{\text{ext}}^{(R)} = \text{Re } q_{\text{ext}}(t)$. Furthermore, we have introduced the quantities

$$M_l(\omega) = \text{Re } \mathcal{B}_l(x) - \frac{1}{\omega}\text{Im } \mathcal{Z}_l(x), \quad (4.2)$$

$$C_l(\omega) = \text{Re } \mathcal{C}_l(x) = C_l^{(S)} + \text{Re } \mathcal{C}_l^{(\mu)}, \quad (4.3)$$

$$\gamma_l(\omega) = \text{Re } \mathcal{Z}_l(x) + \omega\text{Im } \mathcal{B}_l(x) - \frac{1}{\omega}\text{Im } \mathcal{C}_l(x), \quad (4.4)$$

which will serve as the basis to define transport coefficients for the inertia, stiffness, and friction, respectively.

As it stands Eq. (4.1) is correct for frequency-dependent $M_l(\omega), \gamma_l(\omega)$, and $C_l(\omega)$. However, we have to remember that our equations have been derived for a strictly harmonic function $Q(t)$ as given by Eq. (2.2). This is consistent with Eq. (4.1) only if we replace these frequency-dependent functions by constants.

With constant transport coefficients the interpretation of the various terms in Eq. (4.1) is easy. The term in the square brackets just represents the collective energy. The term proportional to the friction coefficient γ_l is the change of heat associated with the "nucleonic" degrees of freedom. The right-hand side measures the work done per unit time by the external force, for normal displacements of the surface. To define these constants various procedures are possible.

(1) *Zero frequency limit.* For instance, in cranking-model-type approximations one assumes the collective motion to be sufficiently slow such that the transport coefficients can be evaluated in the "zero-frequency" limit, namely, at $\omega = 0$. Applying this procedure here for temperatures $T \neq 0$ we obtain for the inertia M_l and stiffness C_l coefficients the values of the classic hydrodynamic model, namely,

$$M_l(0) = \frac{1}{l}m\rho_0 R_0^5 \equiv M_l^{\text{LD}}, \quad (4.5)$$

the inertia of irrotational flow, and

$$C_l(0) = C_l^{(S)} \equiv C_l^{\text{LD}}, \quad (4.6)$$

with $C_l^{(S)}$ being the stiffness coefficient of the surface energy.

For friction the situation is slightly different. We get a form for $T \neq 0$,

$$\gamma_l(0) = 2\nu_{\text{LD}}R_0^3(l - 1) = \gamma_l^{\text{LD}}, \quad (4.7)$$

which because of

$$\nu_{\text{LD}} = \frac{3}{10\pi} \frac{\lambda}{\Omega r_0^3} \frac{\tau_0 \Omega}{T^2} \qquad (4.8)$$

has a dependence on temperature typical for hydrodynamics. However, our result differs from the one found in Ref. [3] for the classical liquid drop model of irrotational flow, if only extended to include two-body viscosity. There, for multipole vibrations, friction was found to be given by

$$\gamma_l^{\text{hyd}} = 2\nu_{\text{LD}} R_0^3 (l-1) \frac{2l+1}{l}, \qquad (4.9)$$

which is larger than the result for γ_l^{LD} by a factor of $(2l+1)/l$. As will be explained in Appendix A we obtained Eq. (4.7) from the Rayleigh function [see Eq. (A5)] for a finite liquid drop, accounting for the boundary conditions on the nuclear surface. The difference between the results (4.7) and (4.9) can be traced back to a different treatment of the normal and the tangential components of the momentum flux tensor near the nuclear surface.

We would like to notice that for the temperature $T = 0$ in the zero-frequency limit we have some significant correction to the liquid drop stiffness [see Eq. (4.3)] due to both Fermi-surface distortion and retardation effects. When derived within perturbation theory in the small parameter $1/(\omega\tau)$ (see Ref. [10]), this correction is seen to be proportional to the anisotropy coefficient μ, Eq. (2.22). The coefficient μ has a finite value for $T = 0$ even in the limit $\omega \to 0$, realized for the zero-sound condition,

$$\frac{\zeta(\hbar\omega)^2}{\tau_0} = \frac{1}{\tau} \ll \omega.$$

In this limit we get also finite values for the coefficient of viscosity $\nu(0)$, Eq. (2.23), and for the friction coefficient $\gamma(0)$, Eq. (4.4), at zero temperature.

For later purposes it is convenient to introduce the dimensionless quantities

$$\bar{M}_l = M_l/M_l^{\text{LD}}, \quad \bar{C}_l = C_l/C_l^{\text{LD}}, \quad \bar{\gamma}_l = \gamma_l/\gamma_l^{\text{LD}}. \qquad (4.10)$$

Furthermore, in order to compare (see Sec. V) our results with those of previous calculations of Refs. [37,38], we also introduce the dimensionless quantity

$$\eta = \frac{\gamma_l}{2\sqrt{M_l C_l}}, \qquad (4.11)$$

which characterizes the degree of damping of collective motion.

(2) *Analytic expressions for the low-frequency region.* Above we have given explicit expressions for the transport coefficients in the zero-frequency limit for temperature $T \neq 0$. As a matter of fact it is possible to lift this strict condition and to derive formulas which are valid whenever $\omega \leq S_{\text{LD}}\Omega$, for which we have $|x| < 1$. This condition can be applied to clarify the definition of transport coefficients in terms of the values of the quantities (4.2)–(4.4) taken at $\omega = \omega^{(m)}$, which gives the position of the maximum of the strength function $\chi''(\omega) \equiv \text{Im} \chi(\omega)$ for the low-frequency region; see Appendix B. By making use of an analogous procedure like in the derivation of Eq. (3.24) one gets from Eqs. (4.2)–(4.8), (4.10), and (3.11)–(3.15), with $S_R = \text{Re}S$ and $S_I = \text{Im}S$,

$$\bar{M}_l \simeq 1 - \frac{6(l+1)}{2l+3} \frac{S_R^2 S_I^2}{(S_R^2 + S_I^2)^2}, \qquad (4.12)$$

$$\bar{C}_l \simeq 1 + \frac{9A^{1/3}\lambda}{b_S G_1(l+2)} \left(S_R^2 - S_I^2 - \frac{1}{3}G_0 G_1 \right), \qquad (4.13)$$

and

$$\bar{\gamma}_l \simeq \frac{\nu}{\nu_{\text{LD}}} \simeq 1 - \frac{15}{2G_1} \frac{T^2}{\bar{\omega}\tau_0\Omega} \left[S_R S_I + \frac{2G_1}{15} \frac{\bar{\omega}\tau_0\Omega}{T^2} \right]. \qquad (4.14)$$

The connection to the zero-frequency limit at $T \neq 0$ is easily understood if we realize that for the collision-dominated regime one has [6]

$$S_R S_I = -\frac{2G_1}{15} \frac{\bar{\omega}\tau_0\Omega}{T^2} + \mathcal{O}((\omega\tau)^2), \qquad (4.15)$$

where $\bar{\omega} = \omega/\Omega$.

For the η_l of Eq. (4.11) we then get

$$\eta_l \simeq -\frac{S_R S_I A^{1/6}}{\omega} \sqrt{\frac{27l(l-1)\lambda}{2G_1 b_S(l+2)\bar{M}_l\bar{C}_l}}. \qquad (4.16)$$

It is very interesting to note that for the present model the low-frequency limit for temperatures $T \neq 0$ is so closely related to the hydrodynamic limit. This can easily be understood referring to the form (2.14) for $\tau = \tau(\omega, T)$ and to the position of the first maxima of the strength distribution. This strength distribution is shown explicitly in Fig. 1. Concentrating on the peak at small frequencies we may neglect the ω dependence of τ so that the condition of collision dominance, $\omega\tau \ll 1$, can be rewritten as

$$\frac{\omega\tau_0}{T^2} \ll 1, \qquad (4.17)$$

which is well fulfilled for temperatures of about $T \geq 1$ MeV.

For the case of the high-temperature limit as given by Eq. (4.17), the η_l of Eq. (4.16) may be rewritten as

$$\eta_l \simeq \frac{2}{15} G_1 \frac{\tau_0\Omega}{T^2} A^{1/6} \sqrt{\frac{27l(l-1)\lambda}{2G_1 b_S(l+2)}}. \qquad (4.18)$$

We only have to consider that according to Eq. (2.24) we have $|S_I| \ll 1$ and $|S_R^2 - \frac{1}{3}G_0 G_1| \ll 1$.

(3) *Fit by an oscillator response function.* Even in the case of strongly overdamped motion one is able to introduce a differential equation for the collective variable, i.e., to replace frequency-dependent coefficients like the ones of Eq. (4.1) by constants. As shown and applied to in Refs. [12,13,17,37] the problem can be solved by defining the transport coefficients proper through a procedure of

fitting an oscillator response function to selected peaks of the collective response function. Here such a fitting procedure would also be adequate at intermediate temperatures, especially because our response function of Eq. (3.18) has poles ($n = 0$) on the imaginary axis of the ω complex plane similarly to the overdamped case in Refs. [12,13,17,37]. In Appendix B we will discuss this method adopted for the present purpose where we know the position of the poles and we can calculate the residues directly from Eq. (3.18). This allows us to find the parameters of the oscillator response function of Eq. (B1) as an approximation to Eq. (3.18). The transport coefficients are then defined in terms of the parameters found with the help of Appendix B. We shall use this procedure for the poles $n = 0, 1$; see discussion of the results below.

For the overdamped mode the friction coefficient γ_{osc} is related to the rate of damping Γ_0, Eq. (3.24), by

$$\gamma_{\mathrm{osc}} = M_{\mathrm{osc}}\Gamma_{\mathrm{osc}} \approx \frac{C_{\mathrm{osc}}}{\Gamma_0}; \qquad (4.19)$$

see Eqs. (B16) and (B12) and the second equation in (B4). As noted in Sec. III, the overdamped motion corresponds to the collision-dominated regime $|\omega\tau| \ll 1$. In this regime the stiffness C_{osc} is close to the hydrodynamic limit C^{LD}. This is confirmed by the numerical calculations discussed in the next section. So, taking into account the estimate in Eq. (3.24), one obtains

$$\gamma_{\mathrm{osc}} \approx \frac{3}{5\pi}\lambda A\tau \approx \frac{3}{5\pi}\lambda A\frac{\tau_0}{T^2}, \qquad (4.20)$$

for low-frequency region where we can neglect the frequency dependence of τ, Eq. (2.14), for a finite temperature. It can be noted that this formula is identical to the $\gamma_l(0)$ of Eq. (4.7) up to the factor $(l - 1)$. Apparently such a factor has been lost when applying Eq. (3.24) to Eq. (4.19). Also notice that expression (4.7) is valid for underdamped motion whereas expression (4.20) applies to overdamped motion. Using Eq. (4.11), the corresponding effective damping constant η_{osc} is given by

$$\eta_{\mathrm{osc}} = \frac{\omega_{\mathrm{osc}}}{2\Gamma_0}$$

$$= \frac{6A^{1/3}\lambda\omega_{\mathrm{osc}}\tau}{5b_S(l-1)(l+2)} \approx \frac{6A^{1/3}\lambda\omega_{\mathrm{osc}}\tau_0}{5b_S(l-1)(l+2)T^2}, \quad (4.21)$$

where we have used the approximate relation $C_{\mathrm{osc}} \approx C^{\mathrm{LD}}$ and $\omega_{\mathrm{osc}} \approx \sqrt{C^{\mathrm{LD}}/M_{\mathrm{osc}}}$ according to Eq. (B12). We find the quantity ω_{osc} to be fairly independent of temperature; see discussion in Sec. V.

(4) *General method for underdamped poles.* We want also to apply a similar method by just evaluating the expressions (4.2)–(4.4) for transport coefficients at the real part ω_n of the poles (3.20). The physical meaning of such a definition is obvious if a pole is close to the real axis for $\Gamma_n \ll \omega_n$. This definition of the transport coefficients clarifies their relation to the characteristics of the excited mode and will be used below for the description of the underdamped motion.

V. DISCUSSION

In the following we will concentrate on the isoscalar quadrupole vibrations of ^{208}Pb and we will thus omit the index $l = 2$. In Fig. 3 we show the solutions to the dispersion equation (2.24) in the complex plane obtained by varying $\omega\tau$. We get both regimes of zero and first sound in the limiting cases of $\omega\tau \to \infty$ and $\omega\tau \to 0$ (see Refs. [4,10]), where S is close to the real axis, and a continuous transition between these regimes where the imaginary part of S takes on finite negative values.

The solutions to the dispersion equation (2.24) were used to calculate the response function $\chi(\omega)$ given by Eq. (3.18). The imaginary part of the response function, scaled by the factor $C^{(S)}/\kappa^2$ to get the dimensionless quantity

$$\bar{\chi}''(\omega) = \frac{C^{(S)}}{\kappa^2}\chi''(\omega), \qquad (5.1)$$

is shown in the upper part of Fig. 1 as a function of the dimensionless frequency

$$\bar{\omega} = \omega/\Omega, \qquad \hbar\Omega = 44A^{-1/3}\ \mathrm{MeV}\ , \qquad (5.2)$$

with Ω being defined in Eq. (3.21). The different curves show the temperature dependence of the response function. In the lower part of Fig. 1 we show the position of the underdamped poles, found from Eq. (3.20) for $n = 1$. To clarify the correspondence with different collision regimes the dependence of $\omega\tau$ [see Eq. (2.14)] on ω is plotted in Fig. 2 for the temperatures T considered in Fig. 1. The interaction parameters $\mathcal{F}_0 = -0.2$ and $\mathcal{F}_1 = 0.6$ used in our calculations are taken from Ref. [10]. Since our main objective in this work is to study the temperature behavior of the response function, we have used the phenomenological value of $\tau_0 = (30/\Omega)\ \mathrm{MeV}^2$ in (2.14) which reproduces the experimental data for the
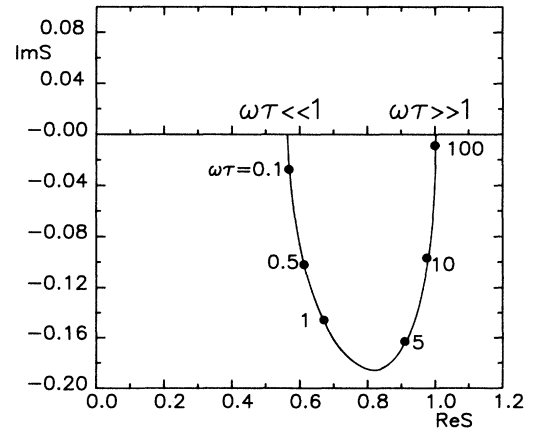
FIG. 3. The sound velocity S, being the complex roots of the dispersion equation (2.24), as a function of $\omega\tau$ with $\mathcal{F}_0 = -0.2$ and $\mathcal{F}_1 = 0.6$.

energy $\hbar\omega_n$ and the width Γ_n of the isoscalar quadrupole resonance of finite nuclei at $T = 0$. Note that microscopic calculations of τ_0 in nuclear matter underestimate the value of Γ_n for cold nuclei; see Ref. [10]. Our results are not very sensitive to the values of the Landau parameters $\mathcal{F}_0$ and $\mathcal{F}_1$ provided that one adopts the limits of $|\mathcal{F}_0| \le 1$ and $|\mathcal{F}_1/3| \ll 1$. It is interesting to note that Fig. 2 shows two hydrodynamic regimes for small and sufficiently large frequencies at temperatures $T \ne 0$ due to the retardation effects related to the ω dependence of the relaxation time τ, Eq. (2.14).

It is seen in Fig. 1 that in the zero-temperature limit only one wide maximum appears at high frequencies. For large temperatures, say, above $T \ge 3$ MeV, only one narrow peak exists but at low frequencies. For temperatures in about the range $0 < T \le 2$ MeV, two maxima are present, one at low frequencies $\omega/\Omega \approx 0.1$ and one at high frequencies $\omega/\Omega \approx 1$. The strengths concentrated in these maxima are redistributed such that the first peak shifts to higher frequencies with temperature and the opposite tendency takes place for the second maximum which is shifted to lower frequency. In the temperature region of about $0 < T \le 3$ MeV the change in the position of the high-frequency resonance is small.

(a) Underdamped motion $(n = 1)$. The high-frequency resonance at $T = 0$, in Fig. 1, can be interpreted as the giant quadrupole resonance because of its energy $\mathcal{E}_1 = \hbar\omega_1$, width $\Gamma_1 = \hbar\Gamma_1$, and its large contribution to the energy-weighted sum rule (EWSR), which agrees with experimental data. This resonance is related to the underdamped mode. The width Γ_1 is due to particle collisions and for the zero temperature comes from the retardation effects.

The results of numerical calculations of the poles for the underdamped excitations, transport coefficients, and degree of damping η are given in Table I. The mass coefficient M is close to the adiabatic hydrodynamic quantity M^{LD}. The stiffness coefficient C for small temperatures is much greater than the liquid drop quantity C^{LD} due to the strong effects of the Fermi-surface distortions. The quantity C decreases monotonously with temperature and approaches the hydrodynamic limit C^{LD} for large temperatures. The effective damping parameter η first increases with temperature T and then decreases, in a way similar to the hydrodynamic law, as T^{-2}; see Eq. (4.18). The magnitude of η is smaller than 1 in correspondence with the underdamped motion. All the definitions of the transport coefficients discussed in Sec. IV give about the same results for low and high temperatures for which the poles are close to the real axis and, hence, to the positions of the strength function maxima [39]. In the intermediate-temperature region where $\Gamma_1 \sim \omega_1$ the definitions discussed here lead to different results.

(b) Overdamped motion $(n = 0)$. The nature of the low-frequency maxima of the strength function at $T \ne 0$ seems to be different than that of the well-known low-lying collective states observed in experiments for cold nuclei. For temperatures of about $0 < T \le 6$ MeV these peaks correspond to the overdamped poles. These poles move from the real axis along the imaginary one following the law $\Gamma_0 \propto T^2$, according to Eq. (3.24), and so the

TABLE I. Transport coefficients (4.10), pole frequencies ($\varpi_1 = \hbar\omega_1$), and dimensionless effective damping parameter (4.11) versus the temperature T for the underdamped mode ($n = 1$). The values of $\bar{M}$, $\bar{C}$, and η were calculated at the frequency $\omega = \omega_1$; $\bar{M}_{osc}$, $\bar{C}_{osc}$, and η_{osc} through the parameters of the oscillator response function (B1); $\bar{M}^{(m)}$, $\bar{C}^{(m)}$, and $\eta^{(m)}$ for the frequency $\omega = \omega^{(m)}$ which corresponds to the maximum of the the strength function (5.1). The parameters of the model are the same as in Fig. 1.

T (MeV)	0	2	4	6	8	10
ϖ_1 (MeV)	10.7	10.0	7.7	3.6	1.9	2.3
ω_1/Ω	1.44	1.35	1.04	0.49	0.26	0.31
Γ_1/Ω	0.38	0.48	0.68	0.70	0.27	0.16
$\bar{M}$	1.1	1.0	1.0	1.0	1.0	1.0
$\bar{C}$	20.9	16.1	4.7	2.0	1.1	1.1
η	0.3	0.4	0.5	0.8	0.6	0.4
$\bar{M}_{osc}$	1.1	0.9	0.009	0.09	0.8	1.0
$\bar{C}_{osc}$	21.1	16.1	0.1	0.6	1.0	1.0
η_{osc}	0.3	0.3	0.6	0.8	0.7	0.4
$\varpi^{(m)}$ (MeV)	10.6	9.3	0.44	1.2	2.0	2.3
$(\omega/\Omega)^{(m)}$	1.43	1.26	0.06	0.16	0.27	0.31
$\bar{M}^{(m)}$	1.1	1.0	1.0	1.0	1.0	1.0
$\bar{C}^{(m)}$	20.9	15.6	1.1	1.1	1.1	1.1
$\eta^{(m)}$	0.3	0.4	2.5	1.1	0.6	0.4

maximum value of the strength function falls off with temperature T.

In Table II we show the transport coefficients and effective damping η for the low-frequency peaks related to the overdamped poles. The result of the numerical calculation for the value of Γ_0 is very close to the analytical solution (3.24) for temperatures of about $0 < T \le 6$ MeV. In the overdamped case we used the definition of the transport coefficients M_{osc}, C_{osc}, and η_{osc} through the parameters of the oscillator response function (B1) as explained in Sec. IV and Appendix B. Table II shows significant differences between the values obtained using this method and the values of Eqs. (4.10) and (4.11) obtained

TABLE II. The same as in Table I for overdamped motion ($n = 0$) except for the transport parameters taken at $\omega = \omega_n$. The microscopic quantities η_{micro} and ϖ_{micro} are taken from Refs. [37,38].

T (MeV)	1	2	3	4	6	8
Γ_0/Ω	0.0035	0.014	0.032	0.058	0.15	0.53
$\bar{M}_{osc}$	0.2	0.2	0.2	0.2	0.2	0.06
$\bar{C}_{osc}$	1.1	1.1	1.1	1.1	1.0	0.6
η_{osc}	116.5	29.1	13.0	7.2	2.8	1.3
$\varpi^{(m)}$ (MeV)	0.03	0.11	0.24	0.44	1.19	2.00
$(\omega/\Omega)^{(m)}$	0.004	0.015	0.033	0.06	0.16	0.27
$\bar{M}^{(m)}$	1.0	1.0	1.0	1.0	1.0	1.0
$\bar{C}^{(m)}$	1.1	1.1	1.1	1.1	1.1	1.1
$\eta^{(m)}$	40.1	10.0	4.4	2.5	1.1	0.6
η_{micro}	0.46	1.63	2.82	4.66		
ϖ_{micro} (MeV)	2.13	1.19	1.12	0.18		

from Eqs. (4.2)–(4.4) in the first maxima of the strength function, at $\omega = \omega^{(m)}$, except for the stiffness coefficient which nearly has the hydrodynamic value. However, the effective damping constant η decreases with temperature approximately by the same law of T^{-2} in both definitions, in correspondence with Eqs. (4.21) and (4.18). Note that the rate Γ_0 of damping of the observed quantities like the mean velocity field (2.17) or particle density (2.18) for the overdamped mode is proportional to τ^{-1} [see Eq. (3.24)], and so increases with temperature T approximately as T^2. Nevertheless, for the friction coefficient γ_{osc} we have $\gamma_{\mathrm{osc}} \propto \Gamma_{\mathrm{osc}} \propto 1/\Gamma_0$ for the most important overdamped pole close to the real axis [see Eq. (4.19)], and according to Eq. (4.20), $\gamma_{\mathrm{osc}} \propto \tau \propto T^{-2}$ for the considered low-frequency region. Here we accounted for the results of Table II which show that the stiffness C_{osc} is almost independent of temperature and $C_{\mathrm{osc}} \approx C^{\mathrm{LD}}$. So for the overdamped mode the temperature dependences of the quantities γ_{osc} and Γ_0 are just opposite to each other.

The temperature dependence of η, denoted by η_{osc} in Table II, is significantly different from the microscopic results of Refs. [37,38] for the effective damping η_{micro}. The microscopic quantity η_{micro} increases with temperature whereas, as noted above, our η_{osc} decreases with temperature. The dependence of η on the temperature obtained in Refs. [37,38] is associated with the disappearance of nuclear shell effects in the stiffness coefficient C and inertia parameter M with increasing temperature. The notable decrease with temperature of the frequency of the first peak in the microscopic calculations of Ref. [12] shown in Table II can be related also to the temperature dependence of the shell effects. As noted above [see comment to Eq. (2.14)], we should take into account also the difference in the definition of the (ω,T) dependence of the relaxation time τ.

Figure 2 shows that for large temperature T we have $\omega\tau \ll 1$ for all ω, and we are close to the first sound regime (see Fig. 3). For small $\omega\tau$ the coefficient μ in

Eq. (2.22), which is related to the Fermi-surface distortions, approaches zero (see Fig. 4). We point out that the transition to classical hydrodynamics is realized in the limit $\mu \to 0$. We thus conclude from Figs. 1–4 that with increasing temperature we have a transition from the zero-sound regime to the first-sound regime and the Fermi-liquid drop model tends to the classical hydrodynamic model [1]. This transition is realized as an underdamped motion.

APPENDIX A: LIQUID DROP VISCOSITY

Let us consider the classical hydrodynamic model for irrotational and incompressible flow. Following Ref. [3] the equation for the energy conservation can be written in the form (4.1) with the friction coefficient given by

$$\gamma_l = \gamma_l^{\mathrm{hyd}} = \nu \int_{\mathcal{V}} d\vec{r}\,\triangle(\bar{u}^2) = 2\nu \oint_{\mathcal{S}} dS \sum_{\beta} \overline{u_\beta} \frac{\partial \overline{u_r}}{\partial r_\beta}. \quad \text{(A1)}$$

Here, $\overline{u_\beta}$ is defined by

$$u_\beta = \overline{u_\beta}\dot{Q}. \quad \text{(A2)}$$

The first integration is to be taken over an arbitrary finite volume $\mathcal{V}$ inside the viscous matter described by the Navier-Stokes equation and the second one is carried out over its surface $\mathcal{S}$. The quantity (A1) was obtained in Ref. [3] from the Rayleigh function [11] which determines the change of the energy concentrated in this volume $\mathcal{V}$ per unit time. Note that for irrotational and incompressible flow the Navier-Stokes equation (2.30) has no viscous terms and according to Eqs. (2.15) and (2.28) the equation of motion is the Laplacian equation. It means that for the dynamics of a finite liquid drop the momentum flux tensor contains viscous components which lead to viscous motion of the liquid drop only due to the boundary conditions like (2.32).

With the help of Eqs. (2.31) and (A2), Eq. (A1) can be rewritten as

$$\gamma_l^{\mathrm{hyd}}\dot{Q}^2 = 2\nu \oint dS u_S \frac{\partial u_r}{\partial r} + 2\nu \sum_{i=1}^{2} \oint dS u_i \frac{\partial u_r}{\partial r_i}$$
$$= -\oint dS u_S \Pi_{rr}^{(\mathrm{dis})} - \sum_{i=1}^{2} \oint dS u_i \Pi_{ri}^{(\mathrm{dis})}, \quad \text{(A3)}$$

FIG. 4. The Fermi-surface distortion coefficient $\bar{\mu} = \mu/(\rho_{\mathrm{eq}}\lambda)$ versus $\omega\tau$ with the same values of $\mathcal{F}_0$ and $\mathcal{F}_1$ as in Fig. 1.

where $\Pi_{\alpha\beta}^{(\text{dis})}$ stands for the dissipative part of the momentum flux tensor (2.20) considered for irrotational and incompressible flow,

$$\Pi_{\alpha\beta}^{(\text{dis})} = 2\nu \frac{\partial u_\alpha}{\partial r_\beta} = -2\nu \frac{\partial^2 \varphi}{\partial r_\alpha \partial r_\beta}. \tag{A4}$$

In Eqs. (A3) and (A4) the index i runs on the tangential components of the quantities in the orthogonal coordinate system $[\beta = (r, i)]$. The first term in Eq. (A3) is related to the work of the dissipative force for normal displacements of the nuclear surface, which we would like to associate with the dissipation energy for a liquid drop,

$$\gamma_l^{\text{LD}} \dot{Q}^2 = 2\mathcal{R} = -\oint dS u_S \Pi_{rr}^{(\text{dis})}. \tag{A5}$$

Here, $\mathcal{R}$ is the Rayleigh function for incompressible irrotational dynamics in a liquid drop of a finite size. This dynamics is described by Eq. (2.30) for motion inside the liquid drop with the boundary conditions (2.31) and (2.32) on its surface. The friction coefficient γ_l^{LD} is exactly the same as derived above in Eq. (4.7). So the difference between our definition of the friction coefficient in Eq. (A5) and the one in Eq. (A3) is related to the work of the dissipative force for tangential displacements of the surface layer of fluid in a liquid drop. Notice that according to the boundary condition (2.32) we are only able to study work done by an external force perpendicular to the surface. As a matter of fact, it does not make sense to attribute work in parallel movements of the surface of a self-bound system like a nucleus. In the end such a movement is determined by the motion of the nucleons themselves.

APPENDIX B: FIT BY AN OSCILLATOR RESPONSE FUNCTION

Let us approximate the selected peak of the response function $\chi''(\omega)$ of Eq. (3.18) which is related to a given nth pair of poles by the oscillator response function $\chi_{\text{osc}}''(\omega) = \text{Im}\,\chi_{\text{osc}}(\omega)$ in the form [37]

$$\chi_{\text{osc}}(\omega) = -\frac{1}{2M_{\text{osc}}\mathcal{E}_{\text{osc}}}\left(\frac{1}{\omega - \omega_n^+} - \frac{1}{\omega - \omega_n^-}\right), \tag{B1}$$

where

$$\omega_n^\pm = \pm\mathcal{E}_{\text{osc}} - i\frac{\Gamma_{\text{osc}}}{2}, \tag{B2}$$

$$\mathcal{E}_{\text{osc}} = \sqrt{\frac{C_{\text{osc}}}{M_{\text{osc}}} - \left(\frac{\Gamma_{\text{osc}}}{2}\right)^2} = \omega_{\text{osc}}\sqrt{1 - \eta^2}, \tag{B3}$$

$$\eta = \frac{\gamma_{\text{osc}}}{2\sqrt{M_{\text{osc}}C_{\text{osc}}}} = \frac{\Gamma_{\text{osc}}}{2\omega_{\text{osc}}}, \tag{B4}$$

$$\omega_{\text{osc}} = \sqrt{\frac{C_{\text{osc}}}{M_{\text{osc}}}} = \sqrt{\mathcal{E}_{\text{osc}}^2 + \left(\frac{\Gamma_{\text{osc}}}{2}\right)^2}. \tag{B5}$$

To simplify the notations we omit the index n in the parameters of the oscillator response function (B1). In the text we have explained the method which allowed us to calculate both the positions as well as the residues of the poles directly. By comparison with Eq. (B1) this allows one to deduce the transport coefficients of inertia, friction, and stiffness. The position of the poles have been denoted by ω_n and Γ_n in Eq. (3.20) as

$$\omega_n^\pm = \pm\omega_n - i\Gamma_n, \qquad n = 0, 1, \ldots. \tag{B6}$$

For underdamped motion this equation is completely equivalent to Eq. (B2). For overdamped motion the situation is different. Whereas, in Eq. (B2), $\mathcal{E}_{\text{osc}}$ will become purely imaginary, its contribution will be included into the Γ_0 of Eq. (3.20) (see below). Besides the $\omega_n^\pm$ we need an additional quantity in order to be able to determine the values of the three transport coefficients. For instance, one may take the height of the maximum of the strength function located at $\omega^{(m)}$ and the identity

$$\chi''(\omega^{(m)}) = \chi_{\text{osc}}''(\omega^{(m)}). \tag{B7}$$

(a) *For the underdamped case* ($n = 1$, $\eta < 1$) the quantity $\mathcal{E}_{\text{osc}}$ is real. With the first condition (B6) we get $\mathcal{E}_{\text{osc}}$ and Γ_{osc} from Table I and then the frequency ω_{osc} from Eq. (B5) and the effective damping η from Eq. (B4). From the second condition (B7) and Eq. (B1) we obtain the mass parameter M_{osc}. The stiffness C_{osc} can then be found from the first equations in (B5) or (B3). One may check that the parameters $\mathcal{E}_{\text{osc}}$, Γ_{osc}, and M_{osc} are close to those obtained by the method of a least-squares fit of the oscillator strength function $\chi_{\text{osc}}''(\omega)$ of Eq. (B1) to the selected peak in the function $\chi''(\omega)$ of Eq. (3.18), in all cases when we have distinct resonances with maxima corresponding approximately to the real part ω_1 of the pole; see Table I.

Note that for the case $\eta < 1$ we can express $\mathcal{E}_{\text{osc}}$ of Eq. (B3) in terms of Γ_{osc} and the value $\omega^{(m)}$, which corresponds to the maximum of the oscillator strength function $\chi_{\text{osc}}''(\omega)$ of Eq. (B1), as

$$\mathcal{E}_{\text{osc}} = \sqrt{\sqrt{(\omega^{(m)})^2 + \left(\frac{\Gamma_{\text{osc}}}{2}\right)^2}\left(2\omega^{(m)} - \sqrt{(\omega^{(m)})^2 + \left(\frac{\Gamma_{\text{osc}}}{2}\right)^2}\right)}. \tag{B8}$$

We can verify now that the values of the quantities $\mathcal{E}_{\text{osc}} = \omega_1$, $\Gamma_{\text{osc}} = \Gamma_1$, and $\omega^{(m)}$ taken from Table I satisfy the relation (B8) for small and large temperatures when we have a good resonance structure of the strength function, at $\omega_1 \approx \omega^{(m)}$, and that all definitions give approximately the same result.

(b) *For the overdamped motion* $(n = 0,\ \eta > 1)$, $\mathcal{E}_{\text{osc}}$ of Eq. (B3) is purely an imaginary quantity,

$$\mathcal{E}_{\text{osc}} = iE_{\text{osc}},\qquad\text{(B9)}$$

and

$$\omega_0^{\pm} = i(\pm E_{\text{osc}} - \Gamma_{\text{osc}}/2),\qquad\text{(B10)}$$

where

$$E_{\text{osc}} = \sqrt{\frac{\Omega^4}{4(\omega^{(m)})^2} - (\omega^{(m)})^2 - \left(\frac{\Gamma_{\text{osc}}}{2}\right)^2},\qquad\text{(B11)}$$

with the frequency $\omega^{(m)}$ corresponding to the maximum of the strength function of Eq. (B7). Note that Ω in Eq. (B11) appears because in practical calculations related to the fitting procedure it is convenient to rewrite all formulas of this appendix in terms of dimensionless quantities like (5.1) and (5.2). We then find $\omega^{(m)}$ in terms of E_{osc} and Γ_{osc} in units of Ω. Coming back again to dimensional quantities we get Eq. (B11) with explicit Ω on the right-hand side.

The oscillator frequency ω_{osc} for the overdamped mode is

$$\omega_{\text{osc}} = \sqrt{\frac{C_{\text{osc}}}{M_{\text{osc}}}} = \sqrt{\left(\frac{\Gamma_{\text{osc}}}{2}\right)^2 - E_{\text{osc}}^2}.\qquad\text{(B12)}$$

For the overdamped case the first condition (B6) of the considered fitting procedure with the definition (B10) gives

$$\Gamma_0 = \pm E_{\text{osc}} + \Gamma_{\text{osc}}/2.\qquad\text{(B13)}$$

From Eqs. (B11) and (B13) one obtains

$$\Gamma_{\text{osc}} = \Gamma_0 \pm \sqrt{\frac{\Omega^4}{2(\omega^{(m)})^2} - 2(\omega^{(m)})^2 - \Gamma_0^2}.\qquad\text{(B14)}$$

As it is shown in Sec. IV only one pole, Eqs. (3.23) and (3.24), near the real axis in the region of about $\Gamma_0 < \Omega$ exists and is responsible for the low-lying peak in the

strength function $\chi''(\omega)$ of Eq. (3.18) for intermediate temperatures of about $1 < T \leq 6$ MeV. This pole corresponds to Eq. (B13) with a minus sign before E_{osc} ($E_{\text{osc}} > 0$ and $\Gamma_{\text{osc}} > 0$ by definition). Hence, another pole in Eq. (B13) can be far from the real axis with Γ_0 larger than Ω. The latter is confirmed by the procedure of the above mentioned direct fitting by the least-squares method with respect to the parameters E_{osc}, Γ_{osc}, and M_{osc}. Such a procedure results in the values $\bar{E}_{\text{osc}} = E_{\text{osc}}/\Omega \gg 1$, $\bar{\Gamma}_{\text{osc}} = \Gamma_{\text{osc}}/\Omega \gg 1$ such that $\bar{E}_{\text{osc}} \approx \bar{\Gamma}_{\text{osc}}/2$ but E_{osc} is a little smaller than $\Gamma_{\text{osc}}/2$ (for the stable mode). So for Eq. (B13) with the upper sign we have $\Gamma_0 \approx \Gamma_{\text{osc}} \gg \Omega$ and for the lower sign one gets $\Gamma_0 \ll \Gamma_{\text{osc}}$. In the first case the overdamped pole is very far from the real axis and cannot significantly affect the strength function $\chi''_{\text{osc}}(\omega)$ of Eq. (B1). Therefore we neglect the second term in Eq. (B1).

We are interested in the values $\omega^{(m)} \ll \Omega$ and $\Gamma_0 < \Omega$ for the temperatures shown in Table II. In this case when we should choose the $+$ sign in Eq. (B14) to get a positive value for Γ_{osc},

$$\Gamma_{\text{osc}} = \Gamma_0 + \sqrt{\frac{\Omega^4}{2(\omega^{(m)})^2} - 2(\omega^{(m)})^2 - \Gamma_0^2}.\qquad\text{(B15)}$$

Note that from the lower sign of Eq. (B13) and Eq. (B12) we obtain

$$\Gamma_{\text{osc}} = \frac{1}{\Gamma_0}(\omega_{\text{osc}}^2 + \Gamma_0^2) \approx \frac{\omega_{\text{osc}}^2}{\Gamma_0},\qquad\text{(B16)}$$

because $\Gamma_0 \ll \Omega$ for temperatures of about $T \leq 6$ MeV and ω_{osc} is of the order of Ω; see Eq. (B12) and Table II.

With the upper sign in Eq. (B13) and for the low-frequency region $\omega^{(m)} \ll \Omega$ the quantity Γ_0 is then

$$\Gamma_0 \approx \frac{\Omega^2}{\sqrt{2}\omega^{(m)}} \gg \Omega\qquad\text{(B17)}$$

and

$$\Gamma_{\text{osc}} \approx \Gamma_0 \gg \Omega,\qquad\text{(B18)}$$

in accordance with the numerical direct fitting procedure discussed above. Let us come back to Eq. (B15) corresponding to the ω_0^+ in Eq. (B10). Starting with Γ_0 and $\omega^{(m)}$ from Table II we can calculate Γ_{osc} from Eq. (B15) and then E_{osc} from Eq. (B11). Hence, we can find the parameter ω_{osc} from Eq. (B12) and the effective damping η from Eq. (B4) ($\eta > 1$ for the overdamped mode). The calculations of the M_{osc} and C_{osc} are the same as in the previous case (a).

[1] A. Bohr and B. Mottelson, *Nuclear Structure* (W. A. Benjamin, New York, 1975), Vol. 2.

[2] P. J. Siemens and A. S. Jensen, *Elements of Nuclei: Many-body Physics with the Strong Interaction* (Addison-Wesley, Reading, MA, 1987).

[3] R. J. Nix and A. J. Sierk, Phys. Rev. C **21**, 396 (1980).

[4] V. M. Kolomietz, *Local Density Approach for Atomic and Nuclear Physics* (Naukova Dumka, Kiev, 1990).

[5] A. A. Abrikosov and I. M. Khalatnikov, Rep. Prog. Phys. **22**, 329 (1959).

[6] J. Sykes and G. A. Brooker, Ann. Phys. (N.Y.) **56**, 1 (1970).

[7] G. A. Brooker and J. Sykes, Ann. Phys. (N.Y.) **61**, 387 (1970).

[8] V. M. Kolomietz and H. H. K. Tang, Phys. Scr. **24**, 915 (1981).

[9] V. M. Strutinsky, A. G. Magner, and M. Brack, Z. Phys. A **319**, 205 (1984).

[10] V. M. Kolomietz, A. G. Magner, and V. A. Plujko, Z. Phys. A **345**, 131 (1993); **345**, 137 (1993).

[11] H. Lamb, *Hydrodynamics*, 6th ed. (Dover, New York, 1945), Sec. 329.

[12] H. Hofmann, S. Yamaji, and A. S. Jensen, Phys. Lett. B **286**, 1 (1992).

[13] S. Yamaji, H. Hofmann, and R. Samhammer, Nucl. Phys. **A475**, 487 (1988).

[14] A. G. Magner, S. Vydrug-Vlasenko, and H. Hofmann, Nucl. Phys. **A524**, 31 (1991).

[15] H. Hofmann and F. A. Ivanyuk, Z. Phys. A **344**, 285 (1993).

[16] D. Pines and P. Nozieres, *The Theory of Quantum Liquids* (Benjamin, New York, 1966).

[17] W. Nörenberg, Nucl. Phys. **A409**, 191 (1983).

[18] G. F. Bertsch, P. F. Bortignon, and R. A. Broglia, Rev. Mod. Phys. **55**, 287 (1983).

[19] S. Ayik and D. Boiley, Phys. Lett. B **276**, 263 (1992); **284**, 482(E) (1992).

[20] E. M. Lifshitz and L. Pitajevskii, *Physical Kinetics* (Nauka, Moscow, 1978).

[21] A. S. Jensen, J. Leffers, K. Reese, H. Hofmann, and P. J. Siemens, Phys. Lett. **117B**, 5 (1982); R. Alkofer, H. Hofmann, and P. J. Siemens, Nucl. Phys. **A476**, 213 (1988).

[22] G. Bertsch, Nucl. Phys. A **249**, 253 (1975).

[23] G. Holzwarth and G. Eckart, Z. Phys. A **284**, 291 (1978).

[24] H. Sagawa and G. Holzwarth, Prog. Theor. Phys. **59**, 1213 (1978).

[25] T. Yukawa and G. Holzwarth, Nucl. Phys. A **364**, 29 (1981).

[26] K. Ando and S. Nishizaki, Prog. Theor. Phys. **68**, 1196 (1982).

[27] G. Holzwarth and G. Eckart, Nucl. Phys. **A325**, 1 (1979).

[28] G. Eckart, G. Holzwarth, and J. P. Da Providencia, Nucl. Phys. **A364**, 1 (1981).

[29] J. P. Da Providencia and G. Holzwarth, Nucl. Phys. **A398**, 59 (1983).

[30] C. Wong and N. Azziz, Phys. Rev. C **24**, 2290 (1981).

[31] L. P. Brito and C. Da Providencia, Phys. Rev. C **32**, 2049 (1985).

[32] M. Di Toro and V. M. Kolomietz, Z. Phys. A **328**, 285 (1987).

[33] A. G. Magner and V. M. Strutinsky, Z. Phys. A **324**, 633 (1985).

[34] V. M. Strutinsky, A. G. Magner, and V. Yu Denisov, Z. Phys. A **322**, 149 (1985).

[35] B. K. Jennings and A. D. Jackson, Phys. Rep. **7**, 141 (1980).

[36] In general Γ_n has two contributions which are due to the imaginary part of S and due to the boundary conditions, as explained in Ref. [10]. For the overdamped pole the first contribution vanishes identically.

[37] D. Kiderlen, H. Hofmann, and F. A. Ivanyuk, Nucl. Phys. **A550**, 473 (1992).

[38] H. Hoffmann, in Proceedings of the International Conference on Nuclear Structure and Nuclear Reactions at Low and Intermediate Energies (Joint Institute of Nuclear Research, Dubna, 1992), Publication No. E4-93-58, p. 292.

[39] This is relevant also to the direct procedure, adopted in Refs. [12,13,17,23], of fitting the oscillator response function $\chi''_{osc}(\omega)$ of Eq. (B1) to the selected peak of the response function $\chi''(\omega)$ of Eq. (3.18) by the least-squares method.